Frustration effects in antiferromagnets on planar random graphs

Martin Weigel* and Des Johnston†
Department of Mathematics and the Maxwell Institute for Mathematical Sciences, Heriot-Watt University, Edinburgh EH14 4AS, United Kingdom

(Received 1 February 2007; revised manuscript received 14 May 2007; published 3 August 2007)

We consider the effect of geometric frustration induced by the random distribution of loop lengths in the "fat" graphs of the dynamical triangulations model on coupled antiferromagnets. While the influence of such connectivity disorder is rather mild for ferromagnets in that an ordered phase persists and only the properties of the phase transition are substantially changed in some cases, any finite-temperature transition is wiped out due to frustration for some of the antiferromagnetic models. A wealth of different phenomena is observed: While for the annealed average of quantum gravity some graphs can adapt dynamically to allow the emergence of a Néel ordered phase, this is not possible for the quenched average, where a zero-temperature spin-glass phase appears instead. We relate the latter to the behavior of conventional spin-glass models coupled to random graphs.

DOI: 10.1103/PhysRevB.76.054408 PACS number(s): 75.10.Hk, 04.60.Nc

I. INTRODUCTION

Models of random networks and surfaces have received extensive attention in statistical physics and field theory due to their wealth of applications in such diverse fields as the modeling of the internet,[1] spin-glass physics,[2] and quantum gravity.[3] The diversity of applications is reflected in a rather large variety of different graph models considered. Generic random graph and network models include the most general Erdös-Rényi model of n bonds distributed randomly between pairs selected from N vertices, as well as the Barabási-Albert graphs constructed with the preferential attachment rule or the Watts-Strogatz method of interpolating between a regular lattice and a random graph via rewiring of links.[1] These constructions result in variable but *uncorrelated* vertex degrees with graph ensembles fully defined by the coordination number distribution $P(q)$. On the other hand, fixed-degree or k-regular random graphs have also been considered, which are equivalent to the nonplanar or "thin" $\phi^3, \phi^4, \ldots$ Feynman diagrams of a zero-dimensional field theory.[4] While none of these networks feature a well-defined topology allowing for a local geometrical interpretation, a fattening of the thin graph propagators to ribbons yields orientable faces, enabling an interpretation of the graphs as random surfaces of fixed genus. The resulting dynamical triangulations model has been thoroughly studied with matrix model and combinatorial methods in the context of Euclidean quantum gravity.[3] The topological constraint induces spatial correlations in the degree distribution, and the ensemble of graphs is no longer fully determined by $P(q)$. Other ensembles of random graphs of well-defined topology have been studied, for instance, the Poissonian Voronoï-Delaunay tessellations resulting from a generalization of the crystallographic Wigner-Seitz construction to randomly distributed generators.[5]

A lot of effort has been invested in understanding the generic geometrical properties of these graph ensembles. In particular, for the network-type models, dynamical properties have been regularly considered, such as the emergence of a giant component as edges are successively added to the graphs.[1] For the Delaunay and dynamical tessellations with a well-defined topology, genuinely geometrical attributes such as the fractal or Hausdorff dimension and the correlation function of the local degrees have been of most interest.[3,5] As an alternative to direct investigations, these ensembles might be characterized by observing the cooperative behavior of matter variables such as classical Ising spins $s_i = \pm 1$ with Hamiltonian

$$\mathcal{H} = -\sum_{\langle i,j \rangle} J_{ij} s_i s_j, \tag{1}$$

or, more generally, Potts or $O(n)$ spins placed on the graph vertices, assuming ferromagnetic couplings $J_{ij}=J_0>0$. This exercise is also of interest from the inverted point of view of studying the effect of these various types of connectivity disorder on the spin models, being complementary to the canonical case of weak disorder from randomness of the couplings on regular lattices.[6] Graphs without topological constraint are inherently nonlocal and thus effectively infinite dimensional. Consequently, one expects mean-field phase transitions for the ferromagnetic models. These are indeed found for the Erdös-Rényi and k-regular (or thin) random graphs,[2,4,7–10] transforming them into convenient alternatives to treatments on the Bethe lattice or the complete graph, not encumbered with boundary effects. More generally, degree distributions with divergent moments can lead to interesting deviations from mean-field behavior.[11] The effects on surfacelike graphs are less homogeneous. For (uncorrelated) bond disorder, the celebrated Harris criterion[6] predicts a change of critical behavior for cases with a positive specific-heat exponent α. An analogous criterion can be formulated for random graphs, taking into account the spatial correlation of the degree distribution.[12] The predicted change in universality class for virtually all types of matter coupled to dynamical triangulations or fat graphs is in agreement with exact results for percolation[13] and numerical investigations of the Ising and Potts models.[14] For Voronoï-Delaunay tessellations, however, the predicted change of universality class for models with $\alpha>0$ such as the two-dimensional $q=3,4$ Potts and three-dimensional Ising models is not observed numerically.[15,16] It is an open problem why, instead,

these models behave according to their regular lattice critical exponents.

In contrast to this weak-disorder case, the effect of connectivity disorder on models with *antiferromagnetic* interactions is much more profound. The existence of odd-length loops on many of the graphs discussed leads to severe geometric frustration with the possibility of altogether precluding the onset of a long-range ordered phase. Interestingly, however, this problem for random graphs has received very little attention to date,[8] such that the behavior of, e.g., the Ising antiferromagnet for the various cases is unclear. The effect of tuning the amount of frustration on a *regular* lattice has been considered in Ref. 17 for the $\pm J$ Ising model on the triangular lattice, where it was found that a spin-glass phase appears as the concentration p of antiferromagnetic bonds is increased from zero and disappears again as the system comes close to the perfect frustration of the pure antiferromagnet. Some use has been made of k-regular or thin random graphs as an alternative realization of the mean-field limit of spin glasses,[2,7] and in general, one expects the perfect frustration of the effectively infinite-dimensional graphs of the nontopological type to lead to mean-field spin-glass behavior for the antiferromagnet. The less extreme case of fixed-topology graphs is the subject of the present study.

The rest of the paper is organized as follows. Section II discusses the general problem of frustration exerted by graphs of the dynamical triangulation type on antiferromagnets and the annealed and quenched limits for the Ising antiferromagnet coupled to different graph types. The results of Monte Carlo simulations for the annealed case are discussed. In Sec. III, we investigate the quenched limit by means of exact ground-state computations in the framework of a defect-wall calculation, comparing Gaussian and bimodal spin glasses to the antiferromagnet. Finally, Sec. IV contains our conclusions.

II. FRUSTRATION FROM FAT GRAPHS

Dynamical triangulations originate in the discrete approach to Euclidean quantum gravity via a path-integral quantization of the gravitational interaction. The integral over metrics is regularized by a sum over combinatorial manifolds or simplicial complexes.[3] We focus here on the case of two dimensions, where this amounts to a sum over all possible gluings of equilateral triangles to closed, orientable surfaces of a given, for instance, planar or toroidal topology. Graphs of this type are hence constructed by taking a number N_2 of equilateral triangles and connecting them together along their edges at random, such that the resulting graph represents a closed and orientable surface of well-defined topology. In a computer simulation, such graphs can be implemented by the successive application of the "link-flip" move depicted in Fig. 1 to the graph starting, e.g., from a regular hexagonal lattice with periodic boundary conditions. The geometric duals of these triangulations naturally are graphs of fixed degree $k=3$, known as planar ϕ^3 Feynman diagrams in field theory. The planarity constraint necessitates a "fattening" of the usual propagators to ribbons, such that this type of diagrams is often referred to as "fat graphs."[18]

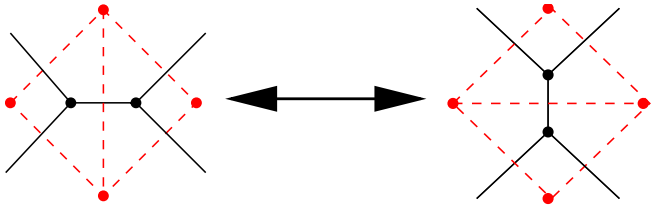

FIG. 1. (Color online) The link-flip move on two adjacent triangles of a dynamical triangulation (dashed lines). The solid lines denote the corresponding dual, three-valent, "fat" ϕ^3 graphs.

Instead of triangles, one can, of course, consider more general elementary polygons, such as the quadrangulations constructed from gluings of squares, whose duals are then consequently "fat" ϕ^4 graphs, etc. The resulting combinatorial problem of counting these discrete surfaces can be solved exactly for various cases using a matrix-model formulation[19] or alternative combinatorial approaches.[20,21] Geometrically, the most striking result is that of an unusually large internal Hausdorff dimension $d_h=4$ for these topologically two-dimensional surfaces,[3] resulting from a structure of "baby universes" connected to the main graph body with a minimal number of links ("bottlenecks"). This fractal structure is apparent from the example graph embedding shown in Fig. 2. While the graphs themselves are, by construction, defined in a purely intrinsic manner, without reference to an embedding into external space, an approximate embedding to some extent observing the constraint of equal edge lengths can be constructed to visualize the internal geometry.[22] The distribution $P(q)$ of coordination numbers is found to fall off exponentially[22,23] and hence does not exhibit the fat tails found in small-world networks. However, the structure of the graphs is not solely determined by $P(q)$, since the well-defined topology introduces long-range correlations in the coordination numbers, declining as r^{-2} at large separations r.[12]

A. Annealed average

When coupling matter variables to the graphs, averages have to be performed for the fluctuations of the graphs as

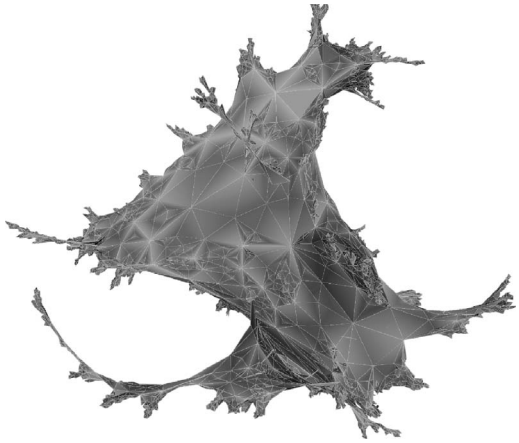

FIG. 2. Example of a dynamical triangulation of $N_2=5000$ triangles embedded into Euclidean space. Note that the equilaterality requirement for the triangles is only approximately fulfilled since an exact embedding into $\mathbb{R}^3$ is not guaranteed to exist.

well as those of the coupled spins with associated characteristic time scales τ_{graph} and τ_{matter}. The *annealed* case of $\tau_{\text{graph}}=\tau_{\text{matter}}$ is the situation considered in the context of matter coupled to quantum gravity. Since spin and disorder degrees of freedom fluctuate on the same time scales, the total free energy of the system is given by

$$F_{\text{annealed}}(\beta) = -\beta^{-1} \ln \langle Z(\beta,\mathcal{G})\rangle_{\mathcal{G}}, \tag{2}$$

where $Z(\beta,\mathcal{G})$ denotes the partition function for spins on a fixed graph $\mathcal{G}$ and $\langle\cdot\rangle_{\mathcal{G}}$ symbolizes the average over the considered graph ensemble. Hence, the effect of geometric randomness on the behavior of spins is augmented by a *backreaction* of matter variables on the underlying graphs. Formulating the combined problem as a multimatrix model, several cases such as the (ferromagnetic) Ising,[24,25] q-state Potts,[26,27] and $O(n)$ models[28,29] (where the two latter classes, of course, include the simpler Ising model as the special cases $q=2$ and $n=1$, respectively) can be treated analytically (in the regime where they show continuous phase transitions on regular lattices, i.e., for $q\leqslant 4$ and $-2\leqslant n\leqslant 2$, respectively). In these cases, the coupling to dynamical triangulations results in a shift of universality class. More generally, in the framework of Liouville theory, Knizhnik, Polyakov, and Zamolodchikov (KPZ) and David, Distler, and Kawai (DDK) predicted the dressing of conformal weights Δ of critical matter coupled to two-dimensional quantum gravity to be[30–32]

$$\tilde{\Delta} = \frac{\sqrt{1-c+24\Delta}-\sqrt{1-c}}{\sqrt{25-c}-\sqrt{1-c}}, \tag{3}$$

where c denotes the central charge.[33] The resulting critical exponents agree with the exact results discussed above, and the predictions for a number of cases have been confirmed by numerical simulation studies, see, e.g., Refs. 34–36.

Coupling *antiferromagnets* to this type of random graphs leads to strong frustration[37] due to the presence of loops of odd length. Depending on the exact type of graphs considered, however, the annealed average to some extent allows for the geometry to adapt to the antiferromagnetic interactions. In particular, consider an Ising antiferromagnet according to Eq. (1), with $J_{ij}=-J_0$ for all bonds, coupled to the following dynamical graphs.

Triangulations. Here, all elementary faces of the graph are frustrated, and the frustration cannot be relieved by a dynamic response of the lattice. As has been shown by Wannier,[38] the Ising antiferromagnet on a *regular* triangular lattice remains paramagnetic down to zero temperature where, due to frustration, the system has a finite residual entropy. It is clear that for any planar triangulation (whether regular or random), configurations of minimal energy have two satisfied and one broken bond in each triangle. A large number of such states exists already for the triangular lattice, which is a member of the ensemble of dynamical triangulations considered. The freedom of changing spin configurations without leaving the ground-state manifold is found to be local, offering no energetic reward and thus precluding long-range order. In fact, the residual, zero-temperature entropy of this model has been calculated[39] to be $S_0\approx 0.2613$, to be compared to the value $S_0\approx 0.3383$ found for the triangular antiferromagnet.[38]

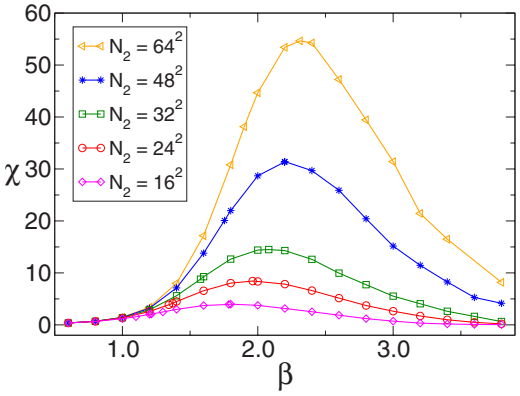

FIG. 3. (Color online) Magnetic susceptibility $\chi=N_2(\langle m^2\rangle-\langle|m|\rangle^2)$ of the Ising antiferromagnet coupled to annealed fat ϕ^3 graphs with $N_2=16^2$ up to $N_2=64^2$ vertices.

Quadrangulations. Any planar quadrangulation is bipartite—it cannot contain any loops of odd length since all loops are composed of the elementary faces of length four. This structure allows for a two-coloring of the lattice vertices in, say, black and white sites. Introducing extra (nonfluctuating) signs $\epsilon_i=\pm 1$ at the vertices and performing a Mattis transformation as[40]

$$s_i' = \epsilon_i s_i, \quad J_{ij}' = J_{ij}\epsilon_i\epsilon_j \tag{4}$$

leaves the Hamiltonian [Eq. (1)] and thus the partition function invariant. Choosing $\epsilon_i^W=-1$ for the white and $\epsilon_i^B=+1$ for the black vertices maps the system identically to the Ising ferromagnet with $J_{ij}=+J_0$. Hence, for the random lattice, the results of Refs. 24 and 25 apply, and the system undergoes a third-order phase transition to a Néel ordered state.

ϕ^3 or ϕ^4 graphs. While neither of these graph classes is bipartite as a whole, it is clear that, e.g., with the hexagonal lattice (ϕ^3 graphs) and the square lattice (ϕ^4 graphs), bipartite graphs occur in both ensembles. Hence, the ground states of either system are perfectly Néel ordered configurations, and it is reasonable to expect long-range order to persist for some finite range of temperatures.

To investigate this last case of a nontrivial interaction between geometric frustration and antiferromagnetism, we performed Monte Carlo simulations of the coupled system for graph sizes of $N_2=16^2-128^2$ vertices. As the temperature is lowered, we indeed find the emergence of antiferromagnetic Néel order with signatures of a phase transition at rather low temperatures $\beta_c\approx 2.5$ (see the susceptibility data shown in Fig. 3). This temperature is to be compared with the phase transition at $\beta_c=\frac{1}{2}\ln\frac{108}{23}\approx 0.773$ found for the Ising *ferromagnet* on the "fat" ϕ^3 graphs without self-energy and tadpole insertions considered here.[25] We find the specific heat to be completely independent of system size with a broad peak around $\beta\approx 1.4$ (see Fig. 4), and no crossing of the Binder parameter within the temperature range $0.1\leqslant\beta\leqslant 4.0$ considered. These findings, together with the apparent scaling of the susceptibility on the low-temperature side of the peak seen in Fig. 3, hint at the presence of a critical (low-

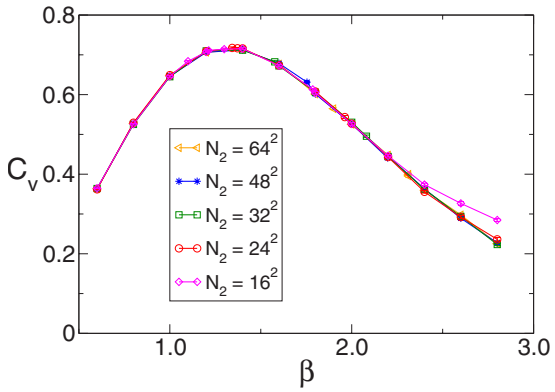

FIG. 4. (Color online) Specific heat $C_v = N_2\beta^2(\langle e^2\rangle - \langle e\rangle^2)$ of the Ising antiferromagnet coupled to annealed fat ϕ^3 graphs from Monte Carlo simulations.

temperature) phase with an associated Kosterlitz-Thouless phase transition.[41] This conjecture is further supported by the very slow convergence of effective critical temperatures as the system size is increased, compatible with a logarithmic rather than a power-law approach. A series of simulations for the *ferromagnet* on the same lattices performed for comparison, on the other hand, yields $\beta_c = 0.783(7)$, $d_h\nu = 3.3(2)$, and $\gamma/d_h\nu = 0.68(3)$, perfectly compatible with the exact results.[24,25]

The mechanism of the antiferromagnetic transition can be understood from an inspection of the distribution $P(q)$ of loop lengths: As the temperature is lowered, the Ising antiferromagnet forces all odd-length loops out of the system, leading to surfaces completely composed out of faces of even length, i.e., squares, hexagons, octagons, etc. (see Fig. 5). Thus, the backreaction of the antiferromagnetic matter on the graphs drives them into a nonfrustrating phase of bipartite graphs compatible with Néel order. The resulting strong coupling between graphs and matter throughout the whole low-temperature region could plausibly give rise to a critical phase with associated infinite-order phase transition as implied by the simulation results discussed above. This is in contrast to the Ising ferromagnet, where strong interaction between matter and geometry is confined to the vicinity of the critical point.

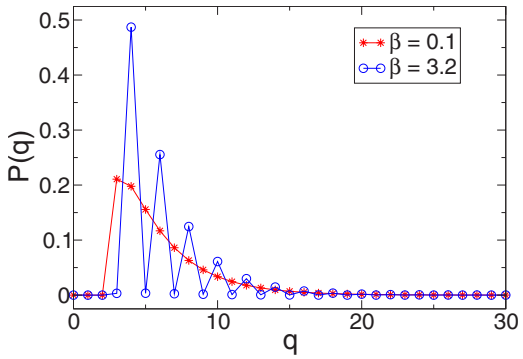

FIG. 5. (Color online) Distribution $P(q)$ of loop lengths of annealed, fat ϕ^3 random graphs coupled to an Ising antiferromagnet in the high-temperature phase at $\beta = 0.1$ and deep in the ordered phase at $\beta = 3.2$. Data are for graphs with $N_2 = 32^2$ vertices.

B. Quenched average

The (graph-) quenched limit $\tau_{\text{graph}} \gg \tau_{\text{matter}}$ of averages describes the case usually encountered in condensed matter physics, where impurities or lattice defects are fixed properties of the sample. Consequently, the average over disorder should be performed at the level of observable quantities, such as the free energy and its derivatives, leading to

$$F_{\text{quenched}}(\beta) = -\beta^{-1}\langle \ln Z(\beta,\mathcal{G})\rangle_{\mathcal{G}}, \tag{5}$$

This interchange of logarithm and disorder average as compared to the annealed limit of Eq. (2) often leads to dramatically different properties. Unfortunately, no exact prediction for ferromagnets in the spirit of Eq. (3) is available here. Since it is believed that ferromagnets with weak quenched disorder in two dimensions, in general, are related to conformal field theories with central charge $c=0$, an approximation starting from the KPZ-DDK framework could be derived from Eq. (3) by setting $c=0$ there,[42] i.e.,

$$\tilde{\Delta} = \frac{1}{4}(\sqrt{1+24\Delta} - 1). \tag{6}$$

This form can also be more directly motivated by noting that the central charge of n replicas of matter variables is additive, such that the limit $n \to 0$ of the replica trick naturally leads to a central charge $c=0$ in Eq. (3).[43–45] These predictions cannot be confronted with any exact solutions. Monte Carlo simulations for the Ising and Potts ferromagnets on quenched dynamical triangulations[14,46] show a change in universality class, in agreement with the adapted relevance criterion for connectivity disorder discussed above.[12] The critical exponents, however, although changed from their regular lattice values, in general, seem not to be correctly predicted by the form (6).

For the antiferromagnets, frustration from quenched, fat graphs is potentially stronger than in the annealed case: The frozen-in disorder of the graphs cannot adapt to alleviate the energy cost of odd-length loops. As before, the degree of frustration exerted on the Ising antiferromagnet depends on the ensemble of graphs considered.

Triangulations. Following the argumentation presented above, the system is paramagnetic at all temperatures for each fixed random triangulation. Consequently, the quenched average merely describes the modulation of a completely disordered system.

Quadrangulations. The perfect bipartiteness of the graphs is not affected by the process of the disorder average. Via the described Mattis transformation, the system is identical to the Ising ferromagnet on quenched quadrangulations. By universality, the critical behavior is expected to be that of the Ising ferromagnet on quenched fat ϕ^3 graphs studied in Ref. 14.

ϕ^3 or ϕ^4 graphs. This graph ensemble features a broad distribution of odd-length loops exerting strong frustration on the coupled antiferromagnet. The lack of a backreaction of the Ising spins on the underlying graphs prevents the suppression of loops of odd length observed in the annealed limit. The bipartite graph configurations selected in the low-temperature phase of the latter only occur with vanishing

weight in the quenched average. This appears to preclude the emergence of long-range order at finite temperatures. However, the frozen-in frustration might give rise to *spin-glass order* at zero temperature.

The rest of this paper is devoted to an investigation of the possibility of such spin-glass order for the Ising antiferromagnet on quenched fat ϕ^3 graphs.

III. ZERO-TEMPERATURE PHASE ON QUENCHED FAT GRAPHS

Due to the random distribution of faces of odd (frustrated) and even (unfrustrated) lengths, it is natural to suspect that the Ising antiferromagnet on ϕ^3 fat graphs behaves similarly to a $\pm J$ Edwards-Anderson spin glass on the same lattices. It is not *a priori* clear, however, whether the long-range correlation of coordination numbers[12] might cause any nonuniversal differences between these cases. How can the appearance of spin glass be detected and its properties determined? Generalizing Peierls' argument for the stability of an ordered phase, a droplet-scaling theory for the spin-glass phase can be formulated.[47] The role of the droplet surface (free) energy is then taken on by the *width* $J(L)$ of the distribution of random couplings for a real-space renormalization group decimation at length scale L. In the course of renormalization, $J(L)$ scales as $J(L) \sim L^{\theta_s}$, defining the *spin-stiffness exponent* θ_s. If the system scales to weak coupling, $\theta_s < 0$, spin-glass order is unstable at finite temperature and the system is below its lower critical dimension, with θ_s describing the properties of the *critical* point at temperature $T=0$. On the other hand, $\theta_s > 0$ indicates stability of a spin-glass phase at finite temperature. Numerically, the domain-wall free energy can be determined from the energy difference between ground states of systems with different types of boundary conditions chosen such as to induce a relative domain wall.[47]

A. Method and droplet length scale

Following this program, one requires the generation of a number of statistically independent graph realizations for performing the quenched average. Subsequently, for each realization, ground states of the Ising antiferromagnet should be calculated. An ergodic set of graph updates for dynamical triangulations (and the dual ϕ^3 graphs) is given by the so-called Pachner moves,[22,48] which we employ to generate independent realizations of toroidal topology, starting out from a perfect hexagonal lattice with periodic boundary conditions. Such a toroidal shape is needed to induce excited states by a change of boundary conditions, as indicated above. The Monte Carlo equilibration is done for closed graphs, leaving the task of identifying appropriate loops along which to cut them open. Several possibilities come to mind:

(1) In the original hexagonal lattice, the identification of boundaries is obvious. If, by construction, no link-flip updates are performed on the links crossing a boundary, the toroidal cuts are *fixed* in the equilibrated graphs. This simplicity, however, comes at the expense of strong boundary effects: Due to the large fractal dimension[3] $d_h=4$, each vertex is comparatively closer to one of the boundaries than would be expected for a two-dimensional system.

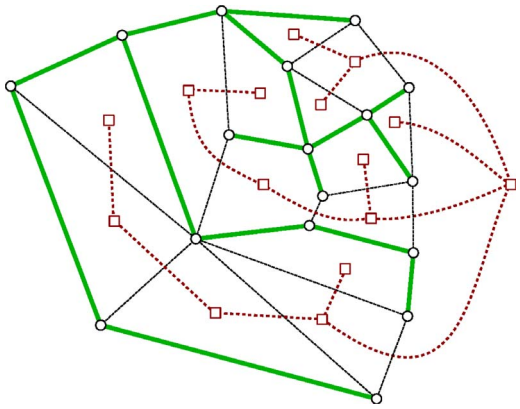

FIG. 6. (Color online) On a planar graph, two interdigitating spanning trees on the original and dual lattices touch or cross all links.

(2) Allowing flips of links crossing a boundary, one might keep track of the induced evolution of the boundary loops. This turns out to be rather involved, in particular, due to the appearance of self-intersections of the meandering boundary lines. Consequently, we have not considered this approach for the final ground-state computations.

(3) Ideally, the graph generation should employ periodic boundary conditions preventing surface effects with the graphs being "cut open" once equilibrated. This amounts to the identification of topologically inequivalent elementary loops on the surface. It is not immediately obvious, however, how such an optimal *homotopy* basis could be computed for an intrinsic graph structure.

As it turns out, a number of computational problems related to topologically motivated cuttings of surfaces are *NP* hard. In particular, identification of the so-called cut graph whose removal renders a surface topologically trivial, i.e., the locus of all points with at least two shortest paths from a given base point, is a nonpolynomial problem.[49] Rather surprisingly, however, a homotopy basis of minimum length in the form of a system of loops joint in a common base point *can* be computed in polynomial time.[50] Such a system consists of $2g$ simple loops (where g is the genus of the surface), whose complement in the manifold is a topological disk. This decomposition proceeds with a variant of the tree-cotree decomposition proposed in Ref. 51: Starting from a marked base point on a planar surface, the dual complement of a spanning tree is a spanning tree as well (see Fig. 6). For nontrivial topology, however, by Euler's formula, both trees simply do not have enough edges to cover the whole graph, and it is easily seen that the edges not touched by either tree are those defining the topologically nontrivial loops with respect to the base point. A set of *minimal* loops can then be found by computing the tree T of shortest paths in the graph G and the maximum spanning tree T^* in the complement $(G \backslash T)^*$, where the weight of each dual edge e^* is chosen to be the length of the shortest loop in G containing the base point as well as the edge e. The desired basis is then given[50] by the minimal loops defined by all edges e neither contained in T nor crossed by T^*.

Exact ground states of the Ising system on the resulting graphs are computed in polynomial time via the mapping to

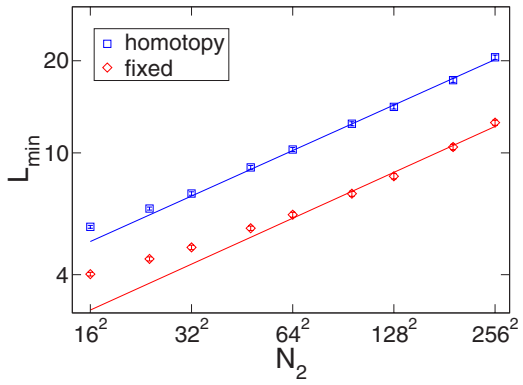

FIG. 7. (Color online) Scaling of the average length $\langle L_{\min}\rangle$ of the domain wall in the *ferromagnet* with antiperiodic boundary conditions, together with fits of the form $\langle L_{\min}\rangle = AN_2^{1/d_h'}$. Note the considerably larger scaling corrections for the graphs with fixed boundaries.

a so-called minimum-weight perfect matching problem.[52] Due to a limitation of this approach, only topologically planar graphs can be treated. Hence, after cutting the graph, one of the resulting boundaries is left open, while either periodic (P) or antiperiodic (AP) conditions are employed along the second boundary. The scaling of the energy difference, $\langle|\Delta E|_{\mathrm{P/AP}}\rangle \sim L_{\mathrm{DW}}^{\theta_s}$, then gives access to the spin-stiffness exponent θ_s. In contrast to the case of a regular lattice, where the relevant domain-wall length scale is simply equivalent to the length of the boundary, $L_{\mathrm{DW}} \sim L$, the corresponding scale is not immediately obvious for the fractal graphs at hand. It can be found, however, from the ground-state problem of the *ferromagnet*: If AP boundary conditions are applied along one direction, the system responds with a domain wall of minimum length $L_{\min}$, corresponding to the length scale of the applied perturbation. The corresponding average length $\langle L_{\min}\rangle$ is shown in Fig. 7 for 5000 graph replicas with $N_2 \leqslant 256^2$. Here, $\langle\cdot\rangle$ denotes an average over disorder. Fits of the form $\langle L_{\min}\rangle = A_L N_2^{1/d_h'}$ yield $d_h'=4.0161(91)$ for the *fixed* boundaries and $d_h'=4.0513(72)$ for the *homotopy* basis, implying that, in fact, $d_h'=d_h=4$, and the relevant domain-wall length scale is equivalent to the intrinsic length $L_{\mathrm{eff}} \sim N_2^{1/d_h}$ of the fractal graphs, implying $\langle|\Delta E|_{\mathrm{P/AP}}\rangle \sim N_2^{\theta_s/d_h}$. Note that the applied fits without correction terms allow an impressively precise determination of d_h, while it turned out to be very tedious to determine the Hausdorff dimension numerically by considering the geometrical two-point function.[22,53]

B. Spin-stiffness exponent

To determine the spin-stiffness exponent θ_s, ground-state computations were performed for a series of graph sizes, comparing the ground-state energies for P and AP boundaries, using 5000 disorder replica for each size. Since previous work has almost exclusively focused on the square lattice,[54] as a benchmark and universality test, we first considered the case of the regular honeycomb lattice, performing fits of the form $\langle|\Delta E|_{\mathrm{P/AP}}\rangle = E_0 + S_E L^{\theta_s}$ for $L=16,24,\ldots,256$. For a Gaussian distribution of the couplings J_{ij} of Eq. (1), we

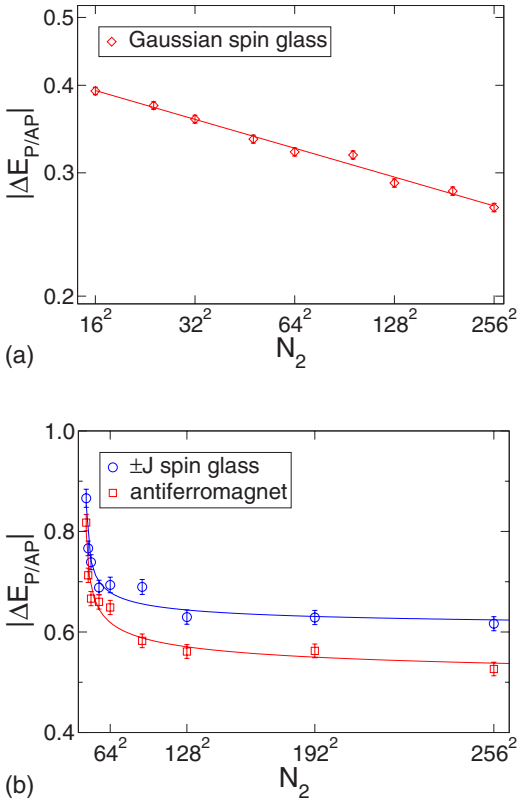

FIG. 8. (Color online) Domain-wall energies of the Gaussian and $\pm J$ Ising spin glasses, as well as the antiferromagnet on quenched, fat ϕ^3 random graphs. The lines show fits of the form $\langle|\Delta E|_{\mathrm{P/AP}}\rangle = E_0 + S_E N_2^{\theta_s/d_h}$ to the data.

arrive at $E_0=0.0026(261)$, clearly indicating that asymptotically, $E_0=0$, as expected. Fixing $E_0=0$ then yields $\theta_s = -0.2843(44)$ with quality of fit $Q=0.29$. This is in excellent agreement with results for the square lattice,[54] the negative value of θ_s indicating that spin-glass order is confined to zero temperature in this system. For symmetric, bimodal couplings $J_{ij}=\pm J$, on the other hand, a clear saturation of defect energies is observed, resulting in $E_0=0.991(15)$, leading to a vanishing $\theta_s=0$ of the effective spin-stiffness exponent. This is again in agreement with the square-lattice result, showing that the $\pm J$ spin glass is marginal in two dimensions (but it turns out that, in fact, $T_g=0$ there),[54] see also Refs. 55–57.

Although the quenched approximation [Eq. (6)] to the KPZ formula [Eq. (3)] has been suggested for unfrustrated situations, it is interesting to see what it predicts for the case at hand. Noting that $\theta_s/d_h = -1/d_h\nu = \Delta_\epsilon - 1$, a dressing according to Eq. (6) yields an invariant $\widetilde{\theta_s/d_h}=0$ for the $\pm J$ model and a renormalized value $\widetilde{\theta_s/d_h}=-0.0886$ from the $\theta_s/d=-0.1422$ found above for the Gaussian bonds. Our results of domain-wall energy computations for ϕ^3 random graphs of sizes $N_2=16^2,24^2,\ldots,256^2$ are collected in Fig. 8, together with fits of the form $\langle|\Delta E|_{\mathrm{P/AP}}\rangle = E_0 + S_E N_2^{\theta_s/d_h}$. As for the honeycomb lattice, the Gaussian spin glass shows clear scaling $\langle|\Delta E|_{\mathrm{P/AP}}\rangle \to 0$, with an estimated $\theta_s/d_h = -0.0684(25)$, different from the ordered lattice case but also not quite compatible with the prediction of the quenched approximation [Eq. (6)]. The $\pm J$ spin glass *and* the antifer-

romagnet show saturation behavior implying $\theta_s/d_h=0$ with $E_0=0.599(23)$ ($\pm J$) and $E_0=0.472(44)$ (antiferromagnet), in agreement with the quenched KPZ prediction. In fact, the finite-size approach is also very similar between these two cases, with essentially only the correction amplitude S_E differing (see Fig. 8). This clearly supports the view that, on the planar random graphs considered here, the antiferromagnet shows zero-temperature spin-glass behavior in the universality class of the $\pm J$ model, in contrast to regular lattices, where the antiferromagnet does not behave like a spin glass.[38]

C. Domain-wall fractal dimension

It has been known for some time that domain walls in spin glasses are fractal curves.[54,58] Recently, evidence has been presented that in two dimensions, they are, in fact, in agreement with the excursions known as "stochastic Loewner evolution," which are closely related to unitary conformal field theories.[59,60] It is interesting to measure the fractal behavior of domain walls on random graphs which are fractals themselves. Considering the link overlap

$$q_l = \frac{1}{N_1}\sum_{\langle i,j\rangle} s_i^{(P)} s_j^{(P)} s_i^{(AP)} s_j^{(AP)} \tag{7}$$

for P and AP boundaries, it is clear that for Ising spins, bonds crossed by a domain wall contribute -1 to q_l, whereas all other bonds contribute $+1$ (N_1 denotes the number of links of the graph). Hence, one expects the scaling

$$\langle 1-q_l\rangle \sim \frac{N_2^{d_s/d_h}}{N_1} \sim N_2^{-(1-d_s/d_h)}, \tag{8}$$

where d_s denotes the fractal dimension of the domain wall (note that $N_1=3N_2/2$ from the Euler formula). For the Gaussian spin glass on the honeycomb lattice, this approach yields $d_s=1.2725(33)$, in good agreement with the accepted value for the square lattice.[54,59,61] (Here, the smallest lattice sizes with $L\leqslant 32$ have been omitted from the fit to account for scaling corrections not explicitly taken into account.) For the bimodal distribution, the comparison of P and AP ground states does not define a unique domain wall due to the high degree of accidental degeneracy in the ground state, such that the above description randomly (but not necessarily without bias) captures one of these walls and a fit to form (8) yields $d_h=1.283(11)$. Note that, hence, there is some uncertainty as to how to define and measure the fractal dimension properly in this case, and consideration of the backbone of ground states,[62] of domain walls of extremal length,[61] or of the residual ground-state entropy[63] leads to different estimates for the square-lattice system. Noting that $d_s/d_h=1-\Delta_{\mathrm{DW}}$, the quenched KPZ approximation [Eq. (6)] predicts $\widetilde{d_s/d_h}=0.4666$ for the Gaussian spin glass coupled to the ϕ^3 random graphs. The numerical results shown in Fig. 9 reveal clear scaling for this case with a resulting estimate $d_s/d_h=0.5042(24)$, again different from the regular lattice value $d_s/d=0.632\,48(88)$, as well as from the quenched KPZ prediction. The corresponding estimates of $d_s/d_h=0.6330(10)$ and $d_s/d_h=0.6425(10)$ for the $\pm J$ and antiferromagnetic models due to degeneracies again refer to some random choice of domain walls. More importantly, however, the scaling approaches for both cases are again almost identical (see Fig. 9), supporting the view of a common universality class for both models.

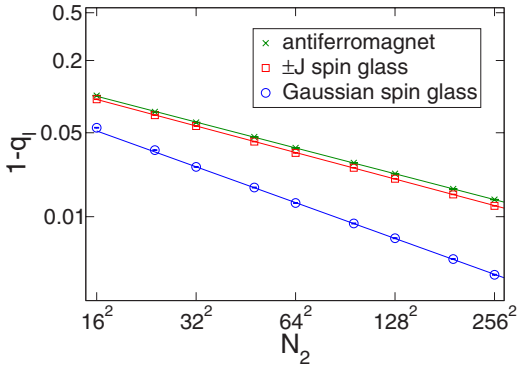

FIG. 9. (Color online) Scaling of zero-temperature domain-wall lengths for the Ising antiferromagnet, as well as the $\pm J$ and Gaussian spin glass on fat ϕ^3 random graphs. The lines show fits of form (8) to the data.

IV. CONCLUSIONS

We have shown that the strongly frustrating influence of odd-length loops present in random graphs can trigger very interesting and characteristic effects in coupled antiferromagnets, with the observed behavior often being very different from that expected for ferromagnets. Only for the special case of bipartite random lattices without odd-length loops such as dynamical quadrangulations does a Mattis transformation identically relate the antiferromagnet to the ferromagnet. The annealed random-graph average considered in quantum gravity allows the lattice to dynamically alleviate frustration, leading, for instance, to the emergence of a Néel ordered phase for the ϕ^3 and ϕ^4 antiferromagnets, apparently accompanied by a Kosterlitz-Thouless phase transition (although, of course, it is not proven that this transition survives in the thermodynamic limit). Quenching the graphs, such dynamical adaptation is precluded, moving the phase transition to zero temperature, where instead a spin-glass phase appears. From an exact defect-wall calculation, it appears that this spin glass is in the same universality class as the $\pm J$ model on the same lattice. The wealth of these observed effects crucially depends on the locality (or finite dimensionality) of the considered surfaces, thus avoiding the possibly less interesting mean-field behavior induced by more generic random graphs.

ACKNOWLEDGMENTS

This work was partially supported by the EC RTN-Network "ENRAGE:" Random Geometry and Random Matrices: From Quantum Gravity to Econophysics, under Grant No. MRTN-CT-2004-005616. M.W. acknowledges support by the EC "Marie Curie Individual Intra-European Fellowships" program under Contract No. MEIF-CT-2004-501422.

*M.Weigel@ma.hw.ac.uk
†D.A.Johnston@ma.hw.ac.uk

[1] R. Albert and A.-L. Barabási, Rev. Mod. Phys. **74**, 47 (2002).
[2] M. Mezard and G. Parisi, J. Stat. Phys. **111**, 1 (2003).
[3] J. Ambjørn, B. Durhuus, and T. Jonsson, *Quantum Geometry—A Statistical Field Theory Approach* (Cambridge University Press, Cambridge, 1997).
[4] C. Bachas, C. de Calan, and P. M. S. Petropoulos, J. Phys. A **27**, 6121 (1994).
[5] A. Okabe, B. Boots, K. Sugihara, and S. N. Chiu, *Spatial Tessallations—Concepts and Applications of Voronoi Diagrams* (Wiley, New York, 2000).
[6] A. B. Harris, J. Phys. C **7**, 1671 (1974).
[7] C. de Dominicis and Y. Goldschmidt, J. Phys. A **22**, L775 (1989).
[8] C. F. Baillie, D. A. Johnston, and J.-P. Kownacki, Nucl. Phys. B **432**, 551 (1994).
[9] D. Johnston and P. Plecháč, J. Phys. A **30**, 7349 (1997).
[10] C. P. Herrero, Phys. Rev. E **65**, 066110 (2002).
[11] A. V. Goltsev, S. N. Dorogovtsev, and J. F. F. Mendes, Phys. Rev. E **67**, 026123 (2003).
[12] W. Janke and M. Weigel, Phys. Rev. B **69**, 144208 (2004).
[13] V. A. Kazakov, Mod. Phys. Lett. A **4**, 1691 (1989).
[14] W. Janke and D. A. Johnston, Nucl. Phys. B **578**, 681 (2000).
[15] W. Janke and R. Villanova, Phys. Rev. B **66**, 134208 (2002).
[16] W. Janke and M. Weigel, Acta Phys. Pol. B **34**, 4891 (2003).
[17] J. Poulter and J. A. Blackman, J. Phys. A **34**, 7527 (2001).
[18] J. Zinn-Justin, *Quantum Field Theory and Critical Phenomena* (Clarendon, Oxford, 1996).
[19] E. Brézin, C. Itzykson, G. Parisi, and J.-B. Zuber, Commun. Math. Phys. **59**, 35 (1978).
[20] W. T. Tutte, Can. J. Math. **14**, 21 (1962).
[21] J. Bouttier, P. Di Francesco, and E. Guitter, Nucl. Phys. B **645**, 477 (2002).
[22] M. Weigel, Ph.D. thesis, University of Leipzig, 2002.
[23] D. V. Boulatov, V. A. Kazakov, I. K. Kostov, and A. A. Migdal, Nucl. Phys. B **275**, 641 (1986).
[24] V. A. Kazakov, JETP Lett. **44**, 133 (1986).
[25] Z. Burda and J. Jurkiewicz, Acta Phys. Pol. B **20**, 949 (1989).
[26] J. M. Daul, arXiv:hep-th/9502014 (unpublished).
[27] P. Zinn-Justin, J. Stat. Phys. **98**, 245 (2000).
[28] M. Gaudin and I. Kostov, Phys. Lett. B **220**, 200 (1989).
[29] B. Eynard and C. Kristjansen, Nucl. Phys. B **455**, 577 (1995).
[30] V. G. Knizhnik, A. M. Polyakov, and A. B. Zamolodchikov, Mod. Phys. Lett. A **3**, 819 (1988).
[31] F. David, Mod. Phys. Lett. A **3**, 1651 (1988).
[32] J. Distler and H. Kawai, Nucl. Phys. B **321**, 509 (1989).
[33] M. Henkel, *Conformal Invariance and Critical Phenomena* (Springer, Berlin, 1999).
[34] J. Jurkiewicz, A. Krzywicki, B. Petersson, and S. Söderberg, Phys. Lett. B **213**, 511 (1988).
[35] C. F. Baillie and D. A. Johnston, Mod. Phys. Lett. A **7**, 1519 (1992).
[36] S. Catterall, J. B. Kogut, and R. L. Renken, Nucl. Phys. B **408**, 427 (1993).
[37] G. Toulouse, Commun. Phys. (London) **2**, 115 (1977).
[38] G. H. Wannier, Phys. Rev. **79**, 357 (1950).
[39] C. Bachas, in *Random Surfaces and Quantum Gravity*, edited by O. Alvarez, E. Marinari, and P. Windey (Plenum, New York, 1991).
[40] D. C. Mattis, Phys. Lett. **56A**, 421 (1976).
[41] M. Weigel and W. Janke, Nucl. Phys. B **719**, 312 (2005).
[42] V. Gurarie and A. W. W. Ludwig, J. Phys. A **35**, L377 (2002).
[43] D. A. Johnston, Phys. Lett. B **277**, 405 (1992).
[44] C. F. Baillie, K. A. Hawick, and D. A. Johnston, Phys. Lett. B **328**, 284 (1994).
[45] W. Janke and D. A. Johnston, Phys. Lett. B **460**, 271 (1999).
[46] W. Janke and D. A. Johnston, J. Phys. A **33**, 2653 (2000).
[47] A. J. Bray and M. A. Moore, in *Heidelberg Colloquium on Glassy Dynamics*, edited by J. L. van Hemmen and I. Morgenstern (Springer, Heidelberg, 1987), p. 121.
[48] V. Pachner, Eur. J. Comb. **12**, 129 (1991).
[49] J. Erickson and S. Har-Peled, Discrete Comput. Geom. **31**, 37 (2004).
[50] J. Erickson and K. Whittlesey, in Proceedings of the 16th Annual ACM-SIAM Symposium on Discrete Algorithms (SIAM, Philadelphia, 2005), p. 1038.
[51] D. Eppstein, in Proceedings of the 15th Annual ACM-SIAM Symposium on Discrete Algorithms (SIAM, Philadelphia, 2004), p. 451.
[52] I. Bieche, R. Maynard, R. Rammal, and J. P. Uhry, J. Phys. A **13**, 2553 (1980).
[53] J. Ambjørn, P. Bialas, Z. Burda, J. Jurkiewicz, and B. Petersson, Phys. Lett. B **342**, 58 (1995).
[54] N. Kawashima and H. Rieger, in *Frustrated Spin Systems*, edited by H. T. Diep (World Scientific, Singapore, 2005), Chap. 9, p. 491.
[55] H. G. Katzgraber and L. W. Lee, Phys. Rev. B **71**, 134404 (2005).
[56] T. Jörg, J. Lukic, E. Marinari, and O. C. Martin, Phys. Rev. Lett. **96**, 237205 (2006).
[57] R. Fisch, J. Stat. Phys. **125**, 789 (2006).
[58] A. J. Bray and M. A. Moore, Phys. Rev. Lett. **58**, 57 (1987).
[59] C. Amoruso, A. K. Hartmann, M. B. Hastings, and M. A. Moore, Phys. Rev. Lett. **97**, 267202 (2006).
[60] D. Bernard, P. Le Doussal, and A. A. Middleton, arXiv:cond-mat/0611433 (unpublished).
[61] O. Melchert and A. K. Hartmann, arXiv:0704.2004 (unpublished).
[62] F. Romá, S. Risau-Gusman, A. J. Ramirez-Pastor, F. Nieto, and E. E. Vogel, Phys. Rev. B **75**, 020402(R) (2007).
[63] R. Fisch, arXiv:cond-mat/0607622, J. Stat. Phys. (to be published).